



CASE REPORT

Treatment of primary hyperparathyroidism in a Miniature Horse using chemical ablation of abnormal parathyroid tissue localized by 3-phase computed tomography

Sarah F. Colmer¹  | Kathryn Wulster¹ | Amy L. Johnson¹ | David G. Levine¹ |
Claire Underwood¹ | Trevor W. Watkins² | Andrew W. Van Eps¹ 

¹Department of Clinical Studies, New Bolton Center, School of Veterinary Medicine, University of Pennsylvania, Kennett Square, Pennsylvania, USA

²Department of Medical Imaging, Princess Alexandra Hospital, Woolloongabba, Queensland, Australia

Correspondence

Andrew W. Van Eps, Department of Clinical Studies, New Bolton Center, School of Veterinary Medicine, University of Pennsylvania, 382 West Street Road, Kennett Square, PA 19348, USA.
Email: vaneps@vet.upenn.edu

Abstract

A 15-year-old Miniature Horse mare with persistently increased plasma calcium (total and ionized) and serum parathyroid hormone concentrations was presented for suspected primary hyperparathyroidism. Ultrasonography of the thyroid region identified an enlarged heterogeneous mass axial to the right thyroid lobe suggestive of an enlarged parathyroid gland, which was further confirmed using sestamibi nuclear scintigraphy and 3-phase computed tomography. Percutaneous ultrasound-guided ethanol ablation of the mass, a method not previously described in the horse, was performed under general anesthesia resulting in rapid normalization of plasma ionized calcium and serum parathyroid hormone concentrations. Ablation of abnormal parathyroid gland tissue may be a suitable alternative to surgical resection in certain cases of primary hyperparathyroidism in the horse.

KEYWORDS

adenoma, equine, ethanol, hypercalcemia, parathyroid hormone

1 | CASE HISTORY

A 15-year-old 102 kg Miniature Horse mare was referred for evaluation after a 6-month history of weight loss. Evaluation on the farm 1 month before presentation identified multiple abnormalities on a serum biochemical profile including increased plasma total calcium concentration (19 mg/dL; reference range [RR], 10.8–13.5 mg/dL) and plasma ionized calcium concentration (2.5 mmol/L; RR, 1.3–1.5 mmol/L) as well as increased serum parathyroid hormone concentration (187.4 pmol/L; RR, 0.6–11 pmol/L) and normal serum parathyroid related peptide (PTH-rp) concentration (0 pmol/L; RR, 0 pmol/L). The

plasma phosphorus concentration was 2 mg/dL (RR, 2–5.1 mg/dL). The mare had a history of pituitary pars intermedia dysfunction (PPID) and was being treated with 250 µg (2.45 µg/kg PO) of pergolide (Boehringer Ingelheim, Ingelheim am Rhein, Germany) once daily. The mare also had a previous episode of mild laminitis.

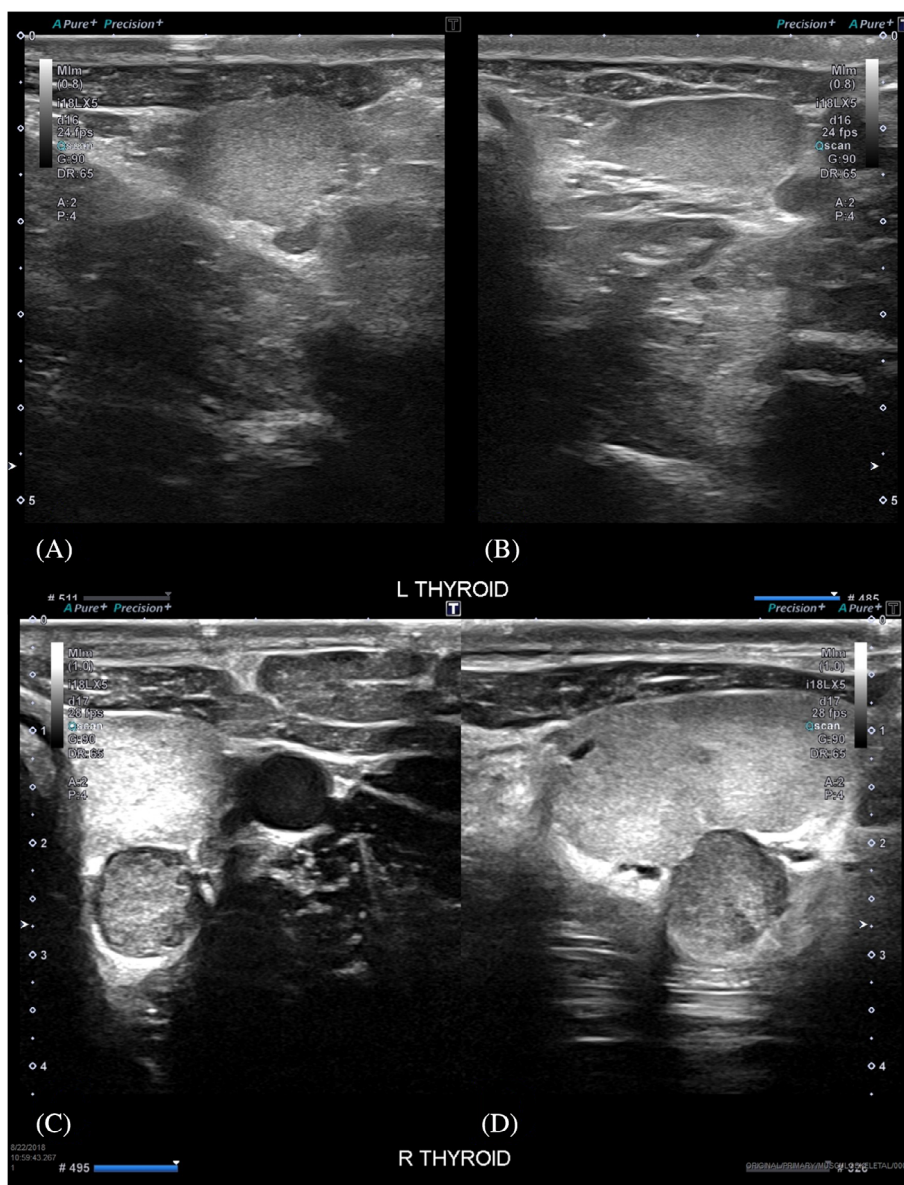
On presentation, body condition score was 4/9 with the ribs slightly visible and decreased topline musculature. Digital pulses were within normal limits. A shortened stride in the hind limbs was evident at the walk, but no overt lameness was present. Palpation of the throatlatch region was unremarkable. A plasma biochemical analysis disclosed increased total calcium (17.79 mg/dL; RR, 10.7–13.4 mg/dL) and normal plasma phosphorus (3.01 mg/dL; RR, 1.9–5.4 mg/dL) concentrations. Radiographs of the metacarpi and metatarsi showed mild generalized osteopenia as evidenced by porosity, mostly affecting the proximal sesamoid bones.

Abbreviations: CT, computed tomography; GGT, gamma-glutamyl transferase; PTH, parathyroid hormone; PTH-rp, parathyroid hormone related peptide; PPID, pituitary pars intermedia dysfunction; ^{99m}Tc, technetium-99m.

This is an open access article under the terms of the Creative Commons Attribution-NonCommercial License, which permits use, distribution and reproduction in any medium, provided the original work is properly cited and is not used for commercial purposes.

© 2022 The Authors. *Journal of Veterinary Internal Medicine* published by Wiley Periodicals LLC on behalf of American College of Veterinary Internal Medicine.

FIGURE 1 Ultrasonography of the thyroid lobes and parathyroid glands at presentation. (A) Transverse image of left thyroid lobe and small $4.6 \times 2.6 \times 3.8$ mm round mass identified axial to the left lobe of the thyroid and presumed to be the left parathyroid gland. (B) Longitudinal image of left thyroid lobe and presumptive parathyroid gland. (C) Transverse image of right lobe of right thyroid lobe and round, discrete hypoechoic mass with a hypoechoic rim that measured $0.98 \times 1.06 \times 1.06$ cm presumed to be the right parathyroid gland. (D) Longitudinal image of right thyroid lobe and presumptive parathyroid gland



On ultrasonography (Aplio i700, Canon Medical Systems USA, Inc, Tustin, CA), the right and left thyroid lobes were homogenous with normal echogenicity, architecture, and size (Figure 1A,B). A discrete hypoechoic mass was present axial to the right thyroid lobe, measuring approximately 1 cm in diameter (Figure 1C). A smaller (approximately 0.4 cm diameter) structure with similar echogenicity was present axial to the left thyroid lobe (Figure 1D). These were suspected to represent parathyroid tissue, with that on the right side markedly increased in size compared to the left. No other masses or abnormalities were observed ultrasonographically.

Technetium (^{99m}Tc) sestamibi scintigraphy was performed to confirm the enlarged parathyroid gland as the site of increased metabolic activity. It also was used to rule out additional sites of ectopic parathyroid tissue, because normal anatomical variation can include a pair of parathyroid glands in the region of the thyroid and an additional caudal pair of parathyroid glands that can vary in location from the bifurcation of the carotid trunk to the ventral aspect of the cranial

third of the neck.¹ A 16-gauge over-the-wire catheter (MILCATH, MILA International, Inc, Florence, KY) was aseptically placed in the right jugular vein and technetium ^{99m}Tc (Technetium99, Pharmalucence, Billerica, MA) was administered (2 mCi/kg IV). At each imaging interval, the mare was treated with 20 mg acepromazine (Covetrus North America, Dublin, OH; 0.02 mg/kg IV), 40 mg xylazine (XylaMed, Bimeda Inc, Oakbrook Terrace, IL; 0.35 mg/kg IV) and 1 mg detomidine (Dormosedan, Zoetis Inc, Parsippany, NJ; 8 $\mu\text{g}/\text{kg}$ IV) for sedation. Images were obtained 10 minutes, 2.5 hours, 5.5 hours, and 24 hours after injection. Initial images identified normal radiopharmaceutical uptake in the parotid salivary glands and a punctate focus of increased radiopharmaceutical uptake just axial to the caudal aspect of the right parotid gland on 10 minute, 2.5 hours, and 5.5 hours images, best visualized on the delayed ventral oblique images (Figure 2).

Three-phase computed tomography (CT) was performed to further characterize the mass axial to the right thyroid lobe. The mare



FIGURE 2 Technetium Tc 99m sestamibi scintigraphy highlighting the parathyroid gland. (A) Right lateral and (B) left lateral ventral oblique images revealing a punctate focus of increased radiopharmaceutical uptake (arrows) just axial to the caudal aspect of the right parotid gland at 2.5 hours after radiopharmaceutical administration

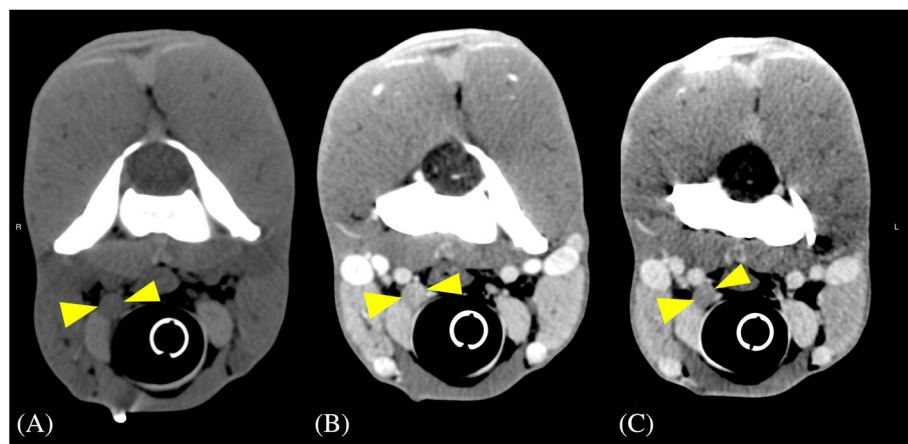


FIGURE 3 Computed tomography (CT) of the ventral neck highlighting the right parathyroid gland at 300 dpi. (A) Baseline CT precontrast exhibiting the parathyroid tissue (arrows) hypoattenuating in relation to the adjacent thyroid tissue. (B) Arterial phase exhibiting comparable attenuation of parathyroid tissue (arrows) to adjacent thyroid tissue. (C) Delayed phase exhibiting hypoattenuation of the parathyroid gland (arrows) in comparison to adjacent thyroid tissue

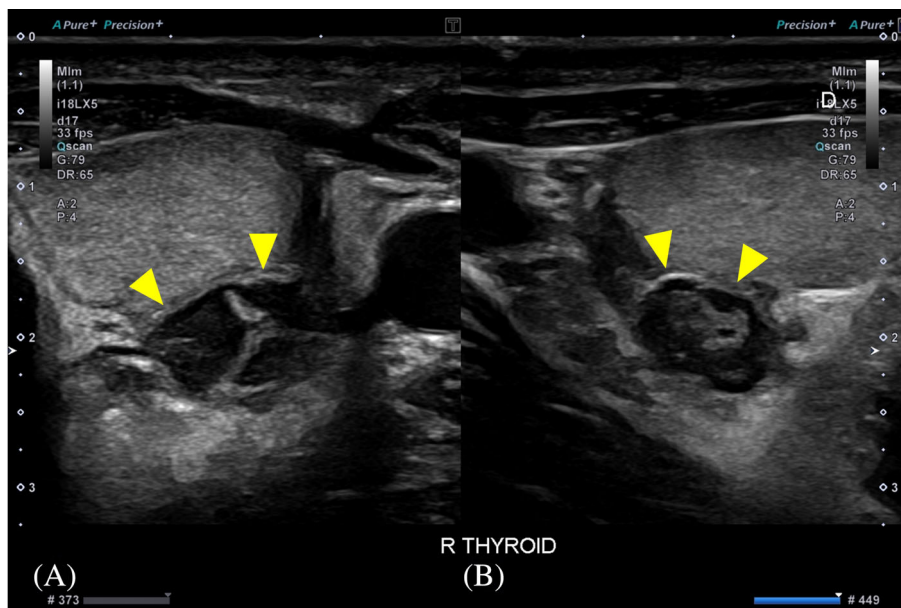
was premedicated with xylazine (XylaMed, Bimeda, Inc, Oakbrook Terrace, IL; 0.5 mg/kg IV) and general anesthesia was induced with midazolam (Midazolam Hydrochloride Injection, West Ward Pharmaceuticals, Eatontown, NJ; 0.09 mg/kg, IV) and ketamine (Ketamine Hydrochloride Injection, Covetrus North America, Dublin, OH; 3 mg/kg IV), and maintained with isoflurane (Isoflurane, Piramal, Mumbai, India) in oxygen in sternal recumbency. Sixty minutes before ablation, blood was collected and submitted for baseline serum PTH (measured at Michigan State University's Veterinary Diagnostic Laboratory, using a validated whole-molecule immunoradiometric assay)² and plasma ionized calcium concentrations which were persistently increased (87.5 pmol/L and 2.08 mmol/L, respectively; Table 1). Pre- and postcontrast arterial and delayed (venous) phase volume data of the region of the nodule and surrounding thyroid tissue were acquired using an 8-slice portable CT scanner (CereTom, NeuroLogica Corporation, Danvers, MA) with axial acquisition (Figure 3) after IV administration of 100 mL (1 mL/kg) IV of 300 mg/mL iohexol (Omnipaque300, GE Healthcare, Chicago, IL) via jugular catheter. The nodule was hypoattenuating relative to thyroid tissue on the precontrast images (Figure 3A), isoattenuating to thyroid tissue on arterial phase images (Figure 3B), and hypoattenuating to thyroid and salivary tissue on delayed phase images (Figure 3C). This attenuation pattern of rapid venous wash out compared to surrounding structures is characteristic of parathyroid adenoma or hyperplasia in humans.^{3,4}

While under general anesthesia, alcohol ablation of the mass dorsal and axial to the right thyroid was performed with the horse in left lateral recumbency. Approximately 1.4 mL of sterile 100% ethanol was injected into the mass using a 2.5" 25-gauge spinal needle (BD Spinal Needle, BD, Franklin Lakes, NJ) under ultrasound guidance. The mare then was hand-recovered. Thirty-five minutes postablation, the serum PTH concentration was normal (4.8 pmol/L; RR, 0.6-11 pmol/L) and plasma ionized calcium concentration had decreased (1.96 mmol/L; RR, 1.58-1.9 mmol/L; Table 1).

Approximately 3 hours postprocedure a further decrease in plasma ionized calcium concentration occurred (1.87 mmol/L; RR, 1.27-1.75 mmol/L). No clinical abnormalities were identified overnight. No palpable heat or swelling was observed in the region where the injection was performed. The plasma ionized calcium concentration had decreased to within normal limits at 21 hours postprocedure (1.58 mmol/L; RR, 1.27-1.75 mmol/L). Repeat ultrasonography of the mass 72 hours postprocedure was consistent with successful ablation of the mass because the homogeneous hypoechoic parenchyma was replaced with hypoechoic fluid and occasional linear echoic strands (Figure 4).

The mare was discharged from the hospital and 6 months later was reportedly doing well with a more comfortable gait and plasma ionized and total calcium concentrations within normal limits at 1.59 mmol/L (RR, 1.58-1.9 mmol/L) and 12.4 mg/dL (RR,

FIGURE 4 Ultrasonography of the right parathyroid gland (arrows) 72 hours postalcohol ablation. (A) Transverse and (B) longitudinal views



10.7-13.4 mg/dL), respectively (Table 1). Eight months postablation serum PTH concentration was mildly increased (17.5 pmol/L; RR, 0.6-11 pmol/L). At 15 months postablation it was further increased (56.6 pmol/L; RR, 0.6-11 pmol/L) but ionized calcium concentration was within normal limits (1.55 mmol/L; RR, 1.58-1.9 mmol/L). The mare returned to our institution for evaluation 16 months after ablation. On ultrasonographic evaluation, the right parathyroid gland was not visualized, and thus repeat ethanol ablation was not pursued. The patient's plasma ionized calcium concentration was 1.65 mmol/dL (RR, 1.27-1.75 mmol/L) and total calcium concentration was 12.62 mg/dL (RR, 10.7-13.4 mg/dL), and because both were normal, the mare was discharged with the recommendation to continue reevaluating serum PTH and total or ionized calcium concentrations every 6 months. At 30 months postprocedure, the serum PTH was normal at 4.4 pmol/L (RR, 0.6-11 pmol/L), the plasma ionized calcium was also normal at 1.77 mmol/L (RR, 1.58-1.9 mmol/L) and the total calcium concentration was normal at 12.2 mg/dL (RR, 10.7-13.4 mg/dL). The mare remained comfortable with no abnormalities on physical examination.

2 | DISCUSSION

We ablated the functional parathyroid tissue in the horse of this report using percutaneous ultrasound-guided ethanol injection, which resulted in rapid and sustained amelioration of hypercalcemia and increased serum PTH. We also used 3-phase contrast CT for detection of parathyroid tissue and procedural planning of parathyroid gland ablation. Although biopsy was not performed before ablation to confirm the nature of the mass, primary hyperparathyroidism due to parathyroid adenoma or hyperplasia was strongly suspected.

Primary hyperparathyroidism is considered uncommon in the horse,⁵ and may be suspected with a combination of clinical signs

such as weight loss, facial swelling, inappetence and shifting lameness.^{6,7} It most often is caused by parathyroid hyperplasia or adenoma of the parathyroid gland and can result from single or multigland disease resulting in overproduction of endogenous PTH.^{8,9} Parathyroid hormone is known to increase plasma calcium concentrations by increased intestinal absorption, decreased renal excretion and increased mobilization of calcium from bone.² In primary hyperparathyroidism, a lack of parathyroid gland response to negative feedback from increasing plasma concentrations of calcium or calcitriol as well as excessive synthesis of PTH are observed.¹⁰

The hypercalcemia observed in this mare included both total and ionized calcium which, coupled with the increased serum PTH concentration, is highly suggestive of primary hyperparathyroidism. Osteopenia of long bones can be seen with primary hyperparathyroidism as a result of mobilization of calcium from bone⁶ and was identified in this mare upon radiography of the metacarpophalangeal and metatarsophalangeal joints. Hypercalcemia also can be observed with pseudohyperparathyroidism or hypercalcemia of malignancy, where neoplastic cells produce proteins with PTH-like effects. No PTH-related peptide was identified in the serum, making pseudohyperparathyroidism an unlikely cause of hypercalcemia in this case. Another condition that can mimic some of the clinical findings observed in this case, including increased serum PTH concentration and weight loss, is nutritional secondary hyperparathyroidism. However, nutritional secondary hyperparathyroidism presents with normocalcemia or hypocalcemia and concurrent hyperphosphatemia.¹¹ Additionally, our mare did not have a history of disproportionate calcium and phosphorous intake or ingestion of oxalates to support secondary hyperparathyroidism.¹²

Cases of primary hyperparathyroidism in humans are most often caused by solitary parathyroid adenomas (80% of cases) or hyperplasia (10%-15% of cases) with the remainder of cases involving multiple gland adenomas or less commonly carcinomas.¹³ In this mare, the

TABLE 1 Concentrations of plasma ionized and total calcium and serum parathyroid hormone concentrations pre- and postalcohol ablation

Variable	60 minutes preablation	35 minutes postablation	3 hours postablation	21 hours postablation	6 months postablation	8 months postablation	15 months postablation	16 months postablation	30 months postablation
Plasma ionized calcium	2.08 (RR 1.58-1.9 mmol/L)	1.96 (RR 1.58-1.9 mmol/L)	1.87 mmol/L (RR 1.27-1.75)	1.56 (RR 1.27-1.75)	1.59 (RR 1.58-1.9 mmol/L)	-	1.55 (RR 1.58-1.9 mmol/L)	1.65 (RR 1.27-1.75 mmol/L)	1.77 (RR 1.58-1.9 mmol/L)
Plasma total calcium	-	-	-	-	12.4 (RR 10.7-13.4 mg/dL)	-	-	12.62 (RR 10.7-13.4)	12.2 (RR 10.7-13.4 mg/dL)
Serum parathyroid hormone	87.5 (RR 0.6-11 pmol/L)	4.8 (RR 0.6-11 pmol/L)	-	-	-	17.5 (RR 0.6-11 pmol/L)	56.60 (RR 0.6-11 pmol/L)	-	4.4 (RR 0.6-11 pmol/L)

Note: Reference ranges (RR) are provided for each value.

ultrasonographically-identified mass dorsal and axial to the right thyroid lobe was presumably the parathyroid gland and was enlarged and heterogenous in comparison to a similar structure axial to the left thyroid. Because horses may have multiple pairs of parathyroid glands, sestamibi nuclear scintigraphy was performed to evaluate for additional ectopic parathyroid tissue along the ventral neck and attempt to confirm the nodule as parathyroid tissue. In humans, sestamibi scintigraphy has a reported sensitivity of 65% and specificity of 88% for localization to side of the neck.¹⁴ Limited information is available for horses, but 10/11 horses with suspected primary hyperparathyroidism were positive on sestamibi scintigraphy in 1 study.¹⁵ The limitations for identification of parathyroid adenoma or hyperplasia in people include the size of the lesion relative to the spatial resolution of nuclear scintigraphy, with improved sensitivity for nodules >500 mg, relative insensitivity and decreased specificity in multigland disease,¹⁶ and relative insensitivity for detection of hyperplasia compared to adenoma.¹⁷ Negative sestamibi scans have accompanied confirmed cases of parathyroid adenomas in horses,⁷ and although our patient had a positive scan, it did not rule out the potential for additional abnormal parathyroid tissue in the region of the proximal neck.

In addition to sestamibi and ultrasonographic imaging, contrast-enhanced CT has been used in human medicine for both diagnosis and preoperative localization of parathyroid adenomas since 2006, with the advent of minimally invasive parathyroidectomy surgery.^{14,18} This scanning method employs CT image acquisition with ≥ 2 contrast material-enhanced phases, resulting in 3-dimensional images, with the fourth dimension being time. The documented contrast enhancement pattern for parathyroid adenomas includes peak enhancement in the arterial phase and washout in the delayed (venous) phase.^{3,14} Although ultrasound provides anatomic localization and sestamibi scintigraphy identifies additional aberrant foci, contrast CT shows excellent detail for preoperative and preprocedural localization, and the appearance of the lesion on different phases can help differentiate parathyroid adenomas and hyperplasia from surrounding lymph nodes or thyroid nodules.^{3,14} Contrast CT as a second-line modality has a reported 70% to 92.5% sensitivity for the localization of parathyroid adenomas to a precise location in the neck with 33% to 46% sensitivity reported for sestamibi imaging and 29% to 38.5% for ultrasound in patients in some studies.^{14,19,20} Additionally, the use of contrast CT has been considered cost-effective in human medicine in comparison to a combination of ultrasound and sestamibi imaging because it provides improved localization for surgical planning as opposed to unsuccessful surgery after neck exploration.^{3,21} The contrast CT performed in our case supported accurate localization of the abnormal parathyroid tissue, which facilitated ablation and minimized the chance of ethanol-associated injury to adjacent structures. The efficiency and speed of contrast CT permitted ablation with minimal preparation and planning and during the same anesthetic event. Contrast CT may be a suitable adjunct to ultrasonography and sestamibi scintigraphy for characterizing abnormal parathyroid tissue in the cranial region of the neck, but size constraints limit the use of CT in the caudal neck of most horses.

Achieving a decrease in circulating serum PTH concentration is imperative in the treatment of primary hyperparathyroidism in order to decrease progression of osteodystrophy and avoid complications such as pathologic fracture and organ calcification. Parathyroidectomy is considered the only curative procedure in humans and is recommended for symptomatic patients as well as individuals with subclinical end-organ sequelae.¹³ Parathyroidectomy is described in the horse, with 1 case study involving removal of a mass at the thoracic inlet resulting in an immediate 95% decrease in serum PTH concentration.⁵ Alternative procedures to parathyroidectomy include ultrasound-guided heat ablation^{22,23} and alcohol ablation,²³ both of which have been successful in dogs.²¹ The benefits of ablation include lower cost, decreased invasiveness and decreased anesthesia time compared to parathyroidectomy.²⁴ In dogs, medical management can be attempted including diuresis to decrease plasma calcium concentration.²⁵ In 1 report, all 7 horses that received medical treatment alone remained hypercalcemic.¹⁵

Complications associated with parathyroidectomy are not well documented in horses, but can include acute kidney injury and hypocalcemic tetany.⁵ In dogs, damage to the recurrent laryngeal nerves and major blood vessels has been documented¹³ and in the mare of this report, close proximity of the mass to the jugular vein, carotid artery and recurrent laryngeal nerve increased the perceived risk of either parathyroidectomy or ablation. It is unclear whether or not ethanol ablation decreases the relative risk of these complications. Hypocalcemia is the most common complication of either treatment in dogs, occurring in approximately 40% of cases after either parathyroidectomy or ablation.^{24,25} The additional risk of fracture inherently associated with general anesthesia also must be considered in horses,²⁶ and an advantage of ablation may be shortened anesthesia time. Prospective studies comparing parathyroidectomy with ablation across species are warranted. In this case, ablation was performed without apparent complication.

The increase in this mare's serum PTH concentration between 8 and 15 months after the procedure possibly was caused by the presence of additional active ectopic parathyroid tissue that was not identified with our imaging modalities, or incomplete success of the ablation procedure. Delayed recurrence of hypercalcemia after ablation has been documented in dogs.²³ Because the previously hyperactive gland was not readily identified and the total and ionized calcium concentrations were normal at follow-up, the mare was discharged with instructions to serially monitor serum PTH and calcium concentrations and these subsequently returned to normal at 30 months postablation without intervention.

In summary, we performed ethanol ablation of the parathyroid gland after localization of abnormal tissue using a combination of ultrasound, scintigraphy, and contrast CT. This procedure was successful with no observed adverse effects. A case series or prospective controlled study may provide confirmation of efficacy of percutaneous ultrasound-guided alcohol ablation for other equids with primary hyperparathyroidism as well as discrete mass identification.

ACKNOWLEDGMENT

No funding was received for this study.

CONFLICT OF INTEREST DECLARATION

Authors declare no conflict of interest.

OFF-LABEL ANTIMICROBIAL DECLARATION

Authors declare no off-label use of antimicrobials.

INSTITUTIONAL ANIMAL CARE AND USE COMMITTEE (IACUC) OR OTHER APPROVAL DECLARATION

Authors declare no IACUC or other approval was needed.

HUMAN ETHICS APPROVAL DECLARATION

Authors declare human ethics approval was not needed for this study.

ORCID

Sarah F. Colmer  <https://orcid.org/0000-0001-7442-8809>

Andrew W. Van Eps  <https://orcid.org/0000-0001-6108-2503>

REFERENCES

1. Krook L, Lowe JE. Nutritional secondary hyperparathyroidism in the horse: with a description of the normal equine parathyroid gland. *Vet Pathol.* 1964;1(1):1-93.
2. Kamr AM, Dembek KA, Reed SM, et al. Vitamin D metabolites and their association with calcium, phosphorus, and PTH concentrations, severity of illness, and mortality in hospitalized equine neonates. *PLoS One.* 2015;10(6):e0127684.
3. Hoang JK, Won-kyung S, Bahl M, et al. How to perform parathyroid 4D CT: tips and traps for technique and interpretation. *Radiology.* 2014;270(1):15-24.
4. Bahl M, Sepahdari AR, Sosa JA, Hoang JK. Parathyroid adenomas and hyperplasia on four-dimensional CT scans: three patterns of enhancement relative to the thyroid gland justify a three-phase protocol. *Rad.* 2015;277(2):454-462.
5. Tomlinson JE, Johnson AL, Ross MW, et al. Successful detection and removal of a functional parathyroid adenoma in a pony using technetium TC 99m sestamibi scintigraphy. *J Vet Intern Med.* 2014;28:687-692.
6. Frank N, Hawkins JF, Couetil LL, et al. Primary hyperparathyroidism with osteodystrophia fibrosa of the facial bones in a pony. *J Am Vet Med.* 1998;212:84-86.
7. Wong D, Sponseller B, Miles K, Butt T, Kersh K, Myers R. Failure of technetium Tc 99m sestamibi scanning to detect abnormal parathyroid tissue in a horse and a mule with primary hyperparathyroidism. *J Vet Intern Med.* 2004;19:589-593.
8. Peauroi JR, Fisher DJ, Mohr FC, et al. Primary hyperparathyroidism caused by a functional parathyroid adenoma in a horse. *J Am Vet Med.* 1998;212(12):1915-1918.
9. Villagran CC, Frank N, Schumacher J, et al. Persistent hypercalcemia and hyperparathyroidism in a horse. *Case Rep Vet Med.* 2014;2014:465425.
10. Benders NA, Junker K, Wensing T, et al. Diagnosis of secondary hyperparathyroidism in a pony using intact parathyroid hormone radioimmunoassay. *Vet Rec.* 2001;149:185-187.
11. Toribio RE. Disorders of the endocrine system. In: Reed SM, ed. *WM Bayly and DC Sellon: Equine Internal Medicine.* 2nd ed. St Louis, MO: WB Saunders; 2004:1295-1327.
12. Cottle HJ, Hughes KJ, Thompson H, Johnston PEJ, Philbey AW. Primary hyperparathyroidism in a 17-year-old Arab x Welsh Cob pony

- mare with a functional parathyroid adenoma. *Equine Vet Educ.* 2016; 28(9):477-485.
13. Walker MD, Silverberg SJ. Primary hyperparathyroidism. *Nat Rev Endocrinol.* 2018;14(2):115-125.
 14. Rodgers SE, Hunter GJ, Hamberg LM, et al. Improved preoperative planning for directed parathyroidectomy with 4-dimensional computed tomography. *Surgery.* 2006;140(6):932-940.
 15. Gorenberg EB, Johnson AL, Magdesian KG, et al. Diagnosis and treatment of confirmed and suspected primary hyperparathyroidism in equids: 17 cases (1999-2016). *Equine Vet J.* 2019;52:83-90.
 16. Nichols KJ, Tomas MB, Tronco GG, Palestro CJ. Sestamibi parathyroid scintigraphy in multigland disease. *Nucl Med Commun.* 2012; 33(1):43-50.
 17. Greenspan BS, Dillehay G, Intenzo C, et al. SNM practice guideline for parathyroid scintigraphy 4.0. *J Nucl Med Technol.* 2012;40(12):111-118.
 18. Wang TS, Cheung K, Farrokhlyar F, et al. Would scan, but which scan? A cost-utility analysis to optimize preoperative imaging for primary hyperparathyroidism. *Surgery.* 2011;150(6):1286-1294.
 19. Hamidi M, Sullivan M, Hunter G, et al. 4D-CT is superior to ultrasound and Sestamibi for localizing recurrent parathyroid disease. *Ann Surg Oncol.* 2018;25:1403-1409.
 20. Yeh R, Tay YKD, Tobacco G, et al. Diagnostic performance of 4D CT and Sestamibi SPECT/CT in localizing parathyroid adenomas in primary hyperparathyroidism. *Rad.* 2019;291:469-476.
 21. Lubitz CC, Stephen AE, Hodin RA, Pandharipande P. Preoperative localization strategies for primary hyperparathyroidism: an economic analysis. *Ann Surg Oncol.* 2012;19(13):4202-4209.
 22. Jiang T, Chen F, Zhou X, Hu Y, Zhao Q. Percutaneous ultrasound-guided laser ablation with contrast-enhanced ultrasonography for hyperfunctioning parathyroid adenoma: a preliminary case series. *Int J Endocrinol.* 2015;2015:673604.
 23. Pollard RE, Long CD, Nelson RW, Hornof WJ, Feldman EC. Percutaneous ultrasonographically guided radiofrequency heat ablation for treatment of primary hyperparathyroidism in dogs. *J Am Vet Med.* 2001;218(7):1107-1110.
 24. Guttin T, Knox VW IV, Diroff JS. Outcomes for dogs with primary hyperparathyroidism following treatment with percutaneous ultrasound-guided ethanol ablation of presumed functional parathyroid nodules: 27 cases (2008-2011). *J Am Vet Med.* 2015;247(7): 771-777.
 25. Rasor L, Pollard R, Feldman EC. Retrospective evaluation of three treatment methods for primary hyperparathyroidism in dogs. *J Am Anim Hosp Assoc.* 2007;43(2):70-77.
 26. Laurenza C, Ansart L, Portier K. Risk factors of anesthesia-related mortality and morbidity in one equine hospital: a retrospective study on 1,161 cases undergoing elective or emergency surgeries. *Front Vet Sci.* 2019;6:514. doi:10.3389/fvets.2019.00514

How to cite this article: Colmer SF, Wulster K, Johnson AL, et al. Treatment of primary hyperparathyroidism in a Miniature Horse using chemical ablation of abnormal parathyroid tissue localized by 3-phase computed tomography. *J Vet Intern Med.* 2022;36(2):798-804. doi:10.1111/jvim.16390